RESEARCH PAPER

Formulation and Characterization of Polyester/Polycarbonate Nanoparticles for Delivery of a Novel Microtubule Destabilizing Agent

Vaibhav Mundra • Yan Lu • Michael Danquah • Wei Li • Duane D. Miller • Ram I. Mahato

ABSTRACT

Purpose Since our newly synthesized potent 5-indolyl derivative, (2-(1 H-Indol-5-yl) thiazol-4-yl) 3, 4, 5-trimethoxyphenyl methanone (LY293), to treat resistant melanoma was hydrophobic, our objective was to synthesize a biodegradable copolymer for formulating this drug into nanoparticles and to determine its anticancer activity and mechanism of action.

Methods Methoxy poly (ethylene glycol)-b-poly (carbonate-co-lactide) [mPEG-b-P (CB-co-LA)] was synthesized for formulating LY293 into nanoparticles by o/w emulsification and stabilization by solvent evaporation. Particle size, drug release profile, *in vitro* efficacy in multiple melanoma cells, and mechanism of action of drug-loaded nanoparticles were determined.

Results LY293-loaded nanoparticles with 170 nm mean size and 2.2 and 4.16% drug loading efficiently inhibited proliferation of A375 and B16F10 cells with IC_{50} of 12.5 nM and 25 nM, respectively. LY293 circumvented multidrug resistance and inhibited proliferation of Pgp overexpressing MDA-MB435/LCC6 MDR1 melanoma cells. Upon treatment with LY293-loaded nanoparticles, A375 cells underwent cell cycle arrest in G2/M phase and apoptotic cell death. Immunofluorescence images showed inhibition of tubulin polymerization after treatment with LY293.

Conclusion LY293-loaded mPEG-b-P (CB-co-LA) nanoparticles showed excellent efficacy and induced apoptosis in melanoma cells. These polyester/polycarbonate-based nanoparticles provided an excellent platform to deliver different poorly soluble drugs to melanoma.

V. Mundra • Y. Lu • M. Danquah • W. Li • D. D. Miller •
R. I. Mahato (✉)
Department of Pharmaceutical Sciences
University of Tennessee Health Sciences Center
19 South Manassas St., CRB Room No 224
Memphis, Tennessee 38103, USA
e-mail: rmahato@uthsc.edu
URL: http://www.uthsc.edu/pharmacy/rmahato

INTRODUCTION

Melanoma is an extremely aggressive type of skin cancer with a high potential of metastasis and ability to develop resistance to most anticancer agents. Metastasis of melanoma is associated with poor prognosis and 5 year survival rate of less than 20% (1,2). Presently dacarbazine and vemurafenib are the only FDA approved small molecules for treating melanoma. However, dacarbazine is associated with a poor response rate of around 7.2–7.5% and has no beneficial effect on long term survival rates (3).

The anticancer effect of most microtubule targeting drugs including paclitaxel and docetaxel are diminished over time due to the development of chemoresistance (4–6). Previously, we had reported the synthesis of a series of 4-substituted methoxybenzoyl-aryl-thiazole (SMART) with good anticancer activity on different cancer cell types (7). These compounds work as microtubule destabilizers by inhibiting tubulin polymerization. Since SMART series of compounds have very poor aqueous solubility (<2 ng/ml), we utilized the structure activity relationship (SAR) based approach to introduce polar and hydrophilic group which resulted in improved aqueous solubility (8). Among them, (2-(1 H-Indol-5-yl) thiazol-4-yl) 3, 4, 5-trimethoxyphenyl methanone (LY293) has shown aqueous solubility of 3 μg/ml which is still not sufficient for systemic administration. Although the use of surfactants like Tween 80 and Cremophor EL significantly increased their solubility, these solubilizing agents are usually associated with liver and kidney toxicity, hemolysis, acute hypersensitivity reaction and peripheral neuropathies (9).

Previously, we had reported that PEG-PLA micelles could improve the aqueous solubility of SMART derivative and bicalutamide (10,11). Although we were able to increase the aqueous solubility of these anticancer agents, we observed only moderate drug loading levels which were not high enough for systemic administration. To solve this problem, we have modified polyester component of the well-established PEG-PLA into polyester/polycarbonate copolymer system using cyclic 5-methyl-5-benzyloxycarbonyl- 1, 3-dioxane-2-one as carbonate monomer (12). Polyester/polycarbonate copolymer improved drug loading levels and reduced critical micellar concentration values. Although mPEG-b-P (CB-co-LA) copolymer of 10,000 Da spontaneously forms micelles, this copolymer is not suitable for preparing nanoparticles due to its low molecular weight and high percentage of mPEG component. To solve this problem, we resynthesized mPEG-b-P (CB-co-LA) copolymer of around 30,000 Da by increasing the molar ratio of carbonate/lactide monomers. We then prepared mPEG-b-P (CB-co-LA) nanoparticles by o/w emulsification and stabilization by subsequent removal of the organic solvent to encapsulate LY293. Following characterization of these formulations in terms of the mean particle size, drug loading and release profiles, we determined their anticancer efficacy in different melanoma cells and mechanism of action.

MATERIALS AND METHODS

Materials

2, 2-Bis (hydroxymethyl) propionic acid, methoxy poly (ethylene glycol) (mPEG, $M_n = 5000$), stannous 2-ethylhexanoate ($Sn(Oct)_2$), dicyclohexylcarbodiimide (DCC), dimethylaminopyridine (DMAP), benzyl bromide and L-lactide were purchased from Sigma Aldrich (St. Louis, MO) and used as received. DMEM medium and Calcein AM were purchased from Invitrogen (Carlsbad, CA). All other reagents were obtained from Sigma–Aldrich (St. Louis, MO) unless otherwise stated and were used as received.

Cell Culture

Human A375 and mouse B16 melanoma cell lines were purchased from American Type Culture Collection (ATCC, Manassas, VA). The Pgp overexpressing multidrug-resistant cell line MDA-MB435/LCC6 MDR1 and the matching sensitive parent cell line were kindly provided by Dr. Robert Clarke (Georgetown University, Washington, DC).

Synthesis and Characterization of LY293

LY293 was synthesized by modifying the A ring of SMART series of analogs as described previously (8). Briefly, THF solution of 3, 4, 5-trimethoxybromobenzene (2.47 mmol) was added to THF solution of n-BuLi (1.6 M, 1.7 mL) under −78°C. The mixture was allowed to stir for 2 h and a solution of Weinreb amide of (R)-N-methoxy-N-methyl-2-(1-(phenylsulfonyl)-1 H-indol-5-yl)-4,5-dihydrothiazole −4-carboxamide (1.24 mmol) was charged (8). The temperature was allowed to increase to RT and stirred overnight followed by quenching of reaction mixture with saturated NH_4Cl. Product was extracted with ethyl ether, and dried with $MgSO_4$. Crude product was refluxed in ethanol solution of 1 N NaOH to obtain the deprotected compound LY293 which was purified by column chromatography to obtain pure compound as a light-yellow solid.

Synthesis of mPEG-b-P (CB-co-LA)

mPEG-b-P(CB-co-LA) was synthesized as reported previously with minor modifications (12). Briefly, benzyl 2, 2-bis (methylol) propionate was first synthesized by reacting 2,2-bis(hydroxymethyl) propionic acid with benzyl bromide at 100°C for 15 h. The product was used to synthesize 5-methyl-5-benzyloxycarbonyl-1, 3-dioxane-2-one by reacting with triphosgene at −78°C in pyridine and dichloromethane. To achieve the targeted molecular weight of about 30,000 Da, mPEG, L-lactide and 5-methyl-5-benzyloxycarbonyl-1, 3-dioxane-2-one having a ratio of 1:2.5:2.5, respectively were reacted in the presence of stannous 2-ethylhexanoate (10 mol% relative to mPEG) as a catalyst at 130°C for 24 h. The crude copolymer was dissolved in chloroform and precipitated in a large amount of diethyl ether and hexane (1:2), filtered and dried under vacuum at the room temperature. Following synthesis, the copolymer was characterized by ^{1}H NMR and GPC. For NMR, chemical shifts were calibrated using tetramethylsilane as reference (0 ppm) and reported as parts per million. For gel permeation chromatography (GPC) narrow polystyrene standards (3600–65000 g/mol) from American polymer standards Corp were used for generating standard curves and the data was processed using LC Solution version 1.21 GPC option software.

Preparation and Characterization of Nanoparticles

Blank and LY293 loaded nanoparticles were prepared by o/w emulsification and subsequent removal of the organic solvent. Briefly, synthesized mPEG-b-P (CB-co-LA) copolymer and drug were dissolved in dichloromethane and acetone mixture (1:1 ratio). Organic phase was added to 1% polyvinyl alcohol solution and emulsified using a Misonix

ultrasonic liquid processor (Farmingdale, NY) at amplitude of 50 for 2 min. Nanoparticles were stabilized by removing organic phase using a rotavapor and recovered by ultracentrifugation at 20,000 rpm for 30 min and washed once with water to remove polyvinyl alcohol and unentrapped drug.

Mean particle size and size distribution of drug-loaded nanoparticles was measured *via* dynamic light scattering (DLS) using a Malvern Zetasizer Nano Series (Worcestershire, UK). Samples were analyzed at the room temperature with a 175° detection angle. Mean nanoparticle size was obtained as a Z-average which is an intensity mean. Particle size is reported as the mean diameter±SD for triplicate samples. Surface morphology and particle size of nanoparticle was determined using a transmission electron microscope (TEM) (JEM-100S Japan). 5 µl of nanoparticles suspension was loaded on a copper grid, followed by blotting of excess liquid and air-dried before negative staining with 1% uranyl acetate. The grid was visualized at 60 kV and magnifications ranging from 50,000X to 100,000X.

Drug loading was estimated by dissolving the lyophilized drug-loaded nanoparticles in dichloromethane and its subsequent evaporation using a rotavapor. Dissolved drug was reconstituted with HPLC mobile phase, centrifuged to remove polymer and thereafter its concentration was measured by reverse phase high performance liquid chromatography (RP-HPLC, Waters, Milford, MA) with a UV detector at 290 nm using a reverse phase C18 column (250 mm×4.6 mm, Alltech, Deerfield, IL). The mobile phase was composed of 65:35 V/V of acetonitrile and water. LY293 concentration was calculated from the peak area according to the following calibration equation: $C = 40.019A - 108.64$ ($R^2 = 0.9987$, lower quantification limit: 114.67 ng/mL). Drug loading was determined by following formula

$$Percentage\ drug\ loading = \frac{weight\ of\ drug}{weight\ of\ nanoparticle} \times 100$$

In Vitro Drug Release from Nanoparticles

The dialysis technique was employed to determine the drug release from mPEG-b-P (CB-co-LA) nanoparticles. mPEG-b-P (CB-co-LA) nanoparticles were placed in a dialysis membrane of 8,000 Da cut-off and dialyzed against 50 mL of 0.1% Tween 80 phosphate buffered saline (PBS) (pH 7.2) in a thermo-controlled shaker with a stirring speed of 180 rpm. Samples of 1 mL were withdrawn at specified times (4, 8, 12, 24, 36, 48, 72, 96, 120, 168 and 216 h) and replaced with fresh media. Release samples were assayed using RP-HPLC as described for drug loading estimation. The cumulative amount of drug released into the media at each time point was evaluated as the percentage of total drug release to the initial amount of the drug. All experiments were performed in triplicate and the data is reported as the mean of the three individual experiments.

Cell Viability Assay

A375, B16F10, MDA-MB435 and MDA-MB435/LCC6 MDR1 cells were cultured in DMEM media supplemented with 10% fetal bovine serum and 1% antibiotic–antimycotic at 37°C in humidified environment of 5% CO_2. Cells were seeded overnight in 96 well plates at a density of 5,000 cells per well and incubated with DMSO solution of LY293 and LY293 nanoparticles for 48 h. At the end of 48 h, cell culture medium was replaced with 100 µL of 0.5 mg/mL 3-(4, 5-dimethyl-thiazol-2-yl)-2, 5-diphenyl tetrazolium bromide (MTT) solution and incubated for 1 h at 37°C. Cell culture medium was removed thereafter and 200 µL of DMSO was added to dissolve the formazan crystals. Absorbance was measured by a microplate reader at a wavelength of 560 nm. Cell viability was expressed as the percentage of the control group. DMSO control and blank nanoparticles were included in all experiments.

Calcein Acetoxymethylester (Calcein AM) Assay

Calcein AM efflux assay was used to determine Pgp inhibition, since Calcein AM is a Pgp substrate, and increase in fluorescence indicates the inhibition of Pgp activity. MDA-MB435 and MDA-MB435/LCC6 MDR1 cells were seeded into black wall clear bottom 96 well plates at a density of 50,000 cells per well a day before the experiment. Media was removed and cells were washed twice with PBS. After treating cells with various concentrations of test compounds in 50 µL of PBS for 15 min at 37°C, 50 µL calcein AM (10 µM) in PBS were added to each well and incubated at 37°C for additional 15 min. To affirm the increase in fluorescence by Pgp inhibition only, Verapamil and Paclitaxel were included as positive and negative controls, respectively. Fluorescent intensity was determined using a SpectraMax M2/M2e spectrofluorometer (Sunnyvale, CA) at the excitation wavelength of 485 nm and emission wavelength of 525 nm.

Propidium Iodide Staining and Cell Cycle Analysis

A375 cells were cultured overnight in a 6 well plate to 80% confluence and then incubated with various formulations for 24 and 48 h. Treated cells were trypsinized and fixed in 70% ice-cold ethanol overnight. After washing with PBS containing RNAse (1 mg/mL), cell pellet was re-suspended in 5 µg/mL propidium iodide staining solution for 15 min at the room temperature. Cell cycle distribution was measured by flow cytometry (Becton, Dickinson, NJ, USA). Results from 10,000 fluorescent events were obtained for cell cycle analysis.

Immunofluorescence Microscopy

A375 cells were cultured in chamber slides for 24 h and then incubated with drug before and after encapsulation into mPEG-b-P (CB-co-LA) nanoparticles for 24 h. Cells were fixed with ice cold methanol and then incubated overnight at 4°C with rabbit monoclonal anti tubulin antibodies. The secondary antibody, Dylight 594 conjugated affinipure donkey anti-rabbit IgG was added and incubated for 1 h. After staining cell nuclei with 1 mg/mL 4′, 6-diamidino-2-phenylindole in PBS, slides were mounted and sealed. Fluorescent images were captured using Zeiss AxioVision fluorescent microscope.

RESULTS

Synthesis and Characterization of LY293

LY293 was synthesized as shown in Fig. 1a and the chemical structure of synthesized LY293 was ascertained by ^{1}H NMR (Fig. 1b), ^{13}C NMR and ESI-MS. ^{1}H NMR (300 M, CDCl3) δ 8.36 (br, s, 1 H), 8.31 (s, 1 H), 8.21 (s, 1 H), 7.92, 7.89 (dd, 1 H, J=1.8, 2.7 Hz), 7.46 (d, 1 H), 7.62 (s, 2 H, J=8.7 Hz), 7.29 (t, 1 H, J=2.7 Hz), 6.64 (br, 1 H), 3.97

(s, 6 H), 3.97 (s, 3 H). MS (ESI) had m/z ratio of 417.1 (M+Na) $^+$ and 392.9 (M - H) $^-$.

Synthesis and Characterization of mPEG-b-P (CB-co-LA)

mPEG-b-P (CB-co-LA) copolymer was synthesized and characterized by ^{1}H NMR and GPC. ^{1}H NMR spectra as shown in (Fig. 2) was used to confirm the polymerization and calculation of molecular weight of the copolymer. The block copolymer molecular weight was calculated based on a comparative analysis of the four methylene protons of PEG (δ=3.65 ppm), one methylene proton of lactide (δ=5.12 ppm) and the five phenyl ring protons (δ=7.3 ppm) observed in the ^{1}H NMR spectrum. From ^{1}H NMR, calculated molecular weight of mPEG$_{114}$-b-P (CB$_{52}$-co-LA$_{147}$) was 28,585 Dalton but when determined by GPC values of 36,000 Daltons and 27,850 Dalton as Mw and Mn were obtained.

Preparation and Characterization of mPEG-b-P (CB-co-LA) Nanoparticles

The mean particle size of mPEG-b-P (CB-co-LA) nanoparticles was 160–170 nm as determined by DLS (Fig. 3a). The
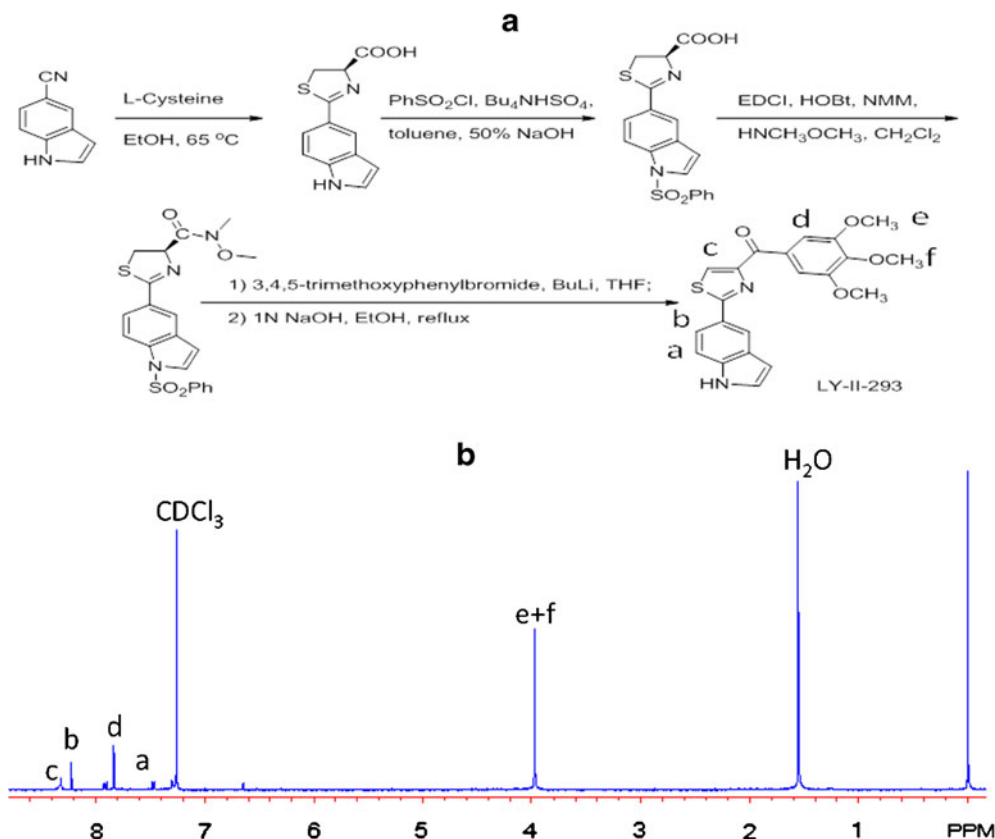

Fig. 1 Synthesis and characterization of 2-(1 H-Indol-5-yl) thiazol-4-yl) 3, 4, 5-trimethoxyphenyl methanone (LY293). (**a**) Synthesis scheme of LY293; (**b**) ^{1}H NMR spectrum of LY293 in CDCl$_3$.
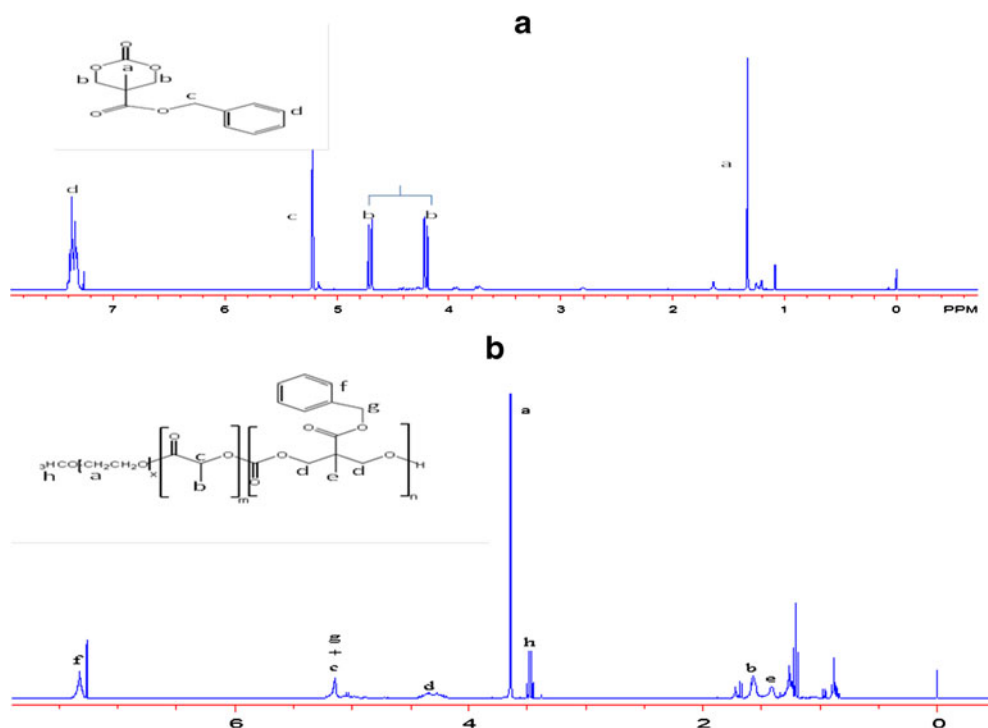
Fig. 2 ^{1}H NMR spectra in CDCl$_3$ of (**a**) 5-methyl-5-benzyloxycarbonyl-1, 3-dioxane-2-one (carbonate monomer) and (**b**) mPEG$_{114}$-b-P (CB$_{52}$-co-LA$_{147}$) copolymer.

morphology and particle size of these nanoparticles was also determined by TEM (Fig. 3b), which showed oval/circular 2D images, with an average diameter of <100 nm. The amount of drug loaded into mPEG-b-P (CB-co-LA) nanoparticles was calculated as drug loading of 2.2 and 4.16% at the theoretical loadings of 2.5 and 5%, respectively (Table I).

The cumulative percentage of LY293 released from mPEG-b-P (CB-co-LA) nanoparticles with two different drug loadings is shown in Fig. 4. These nanoparticles did not show any burst release and less than 10% of drug was released after 10 h (13). Absence of burst release indicated excellent encapsulation of the drug
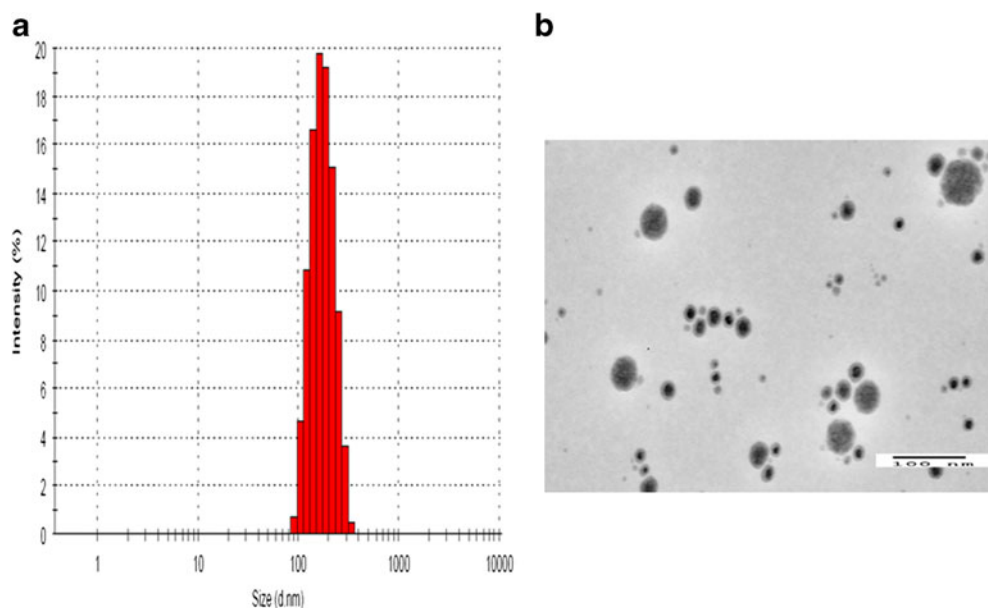

Fig. 3 mPEG-b-P (CB-co-LA) nanoparticle size distribution and morphology. (**a**) Particle size measuring using dynamic light scattering; (**b**) transmission electron micrograph (TEM) obtained using uranyl acetate staining.

Table I Characterization of Drug-Loaded Methoxy Poly (Ethylene Glycol) -b- Poly (Carbonate-co-Lactide) Nanoparticles

Theoretical loading	Drug loading	Particle size	PDI
2.5%	2.2 ± 0.10%	168 ± 10	0.090 ± 0.010
5%	4.16 ± 0.22%	170 ± 10	0.080 ± 0.012

within the nanoparticles and miscibility of drug within the polymeric core. However, 5% drug loaded nanoparticles showed a faster drug release as compared to 2.5% nanoparticles. Similarity factor (f2) was calculated to compare the drug release profiles of 2.5 and 5% drug loaded nanoparticles. The similarity factor was 41.16 for (2.5 vs 5% NP) indicating nanoparticles with two different drug loadings showed different release profiles as the release profiles are considered different when the similarity factor is less than 50 (Fig. 4).

Anti-cancer Activity of Drug-Loaded Nanoparticles

Cytotoxicity of LY293 loaded nanoparticles was determined in A375 and B16F10 melanoma cells. Both DMSO solution of LY293 and drug loaded nanoparticles efficiently inhibited the cancer cell proliferation with an IC_{50} of 25 nM and 100 nm in A375 and B16F10 cells, respectively (Fig. 5). Blank nanoparticles, which had the same polymer concentration as the drug-loaded nanoparticles, did not elicit any cytotoxicity to the cells as expected with biodegradable polymers.

To determine the effect of LY293 in resistant MDA-MB435/LCC6 MDR1 melanoma cells, both MDA-MB435 and resistant MDA-MB435/LCC6 MDR1 cells were incubated with paclitaxel and LY293. MDA-MB435/LCC6 MDR1 is a Pgp overexpressing melanoma

cell line. Cell viability data (Fig. 6) showed that paclitaxel have a resistance index of approximately 100 for the Pgp overexpressing MDA-MB435/LCC6 MDR1 cells. LY293 showed excellent anticancer effect with an IC_{50} of around 8 and 10 nM in MDA-MB435 and resistant MDA-MB435/LCC6 MDR1 cells, respectively, suggesting LY293 is not a substrate of Pgp efflux.

Effect of LY293 on Pgp Activity

To determine the inhibitory activity of LY293 on Pgp, intracellular level of calcein AM (viability dye) was measured by fluorescence spectroscopy. Pgp overexpressing MDA-MB435/LCC6 MDR1 cells were treated with Verapamil, LY293 and paclitaxel. Verapamil is a well-known inhibitor of Pgp activity and leads to intracellular accumulation of calcein AM. LY293 leads to significant intracellular accumulation of calcein AM at a concentration of 5 and 50 μM as compared to untreated and paclitaxel treated cells (Fig. 7).

Effect of LY293 mPEG-b-P (CB-co-LA) Nanoparticles on Cell Cycle and Apoptosis

Tubulin polymerization inhibitors bind to tubulin and arrest the cell cycle in G2/M phase. A375 melanoma cells were treated for 24 and 48 h with DMSO solution of LY293, blank nanoparticles and LY293 nanoparticles to observe the effect of LY293 treatment on cell cycle perturbation. As shown in Fig. 8a, 24 h treatment of A375 cells with DMSO solution of LY293 and LY293 nanoparticles led to cell cycle arrest in G2/M phase while no effect was observed upon treatment with DMSO. Anti-mitotic activity of LY293 lead to increase in G2/M phase from 20.07 ± 2.07% in the

Fig. 4 *In vitro* drug release of LY293 of 2.5 and 5% drug loaded mPEG-b-P (CB-co-LA) nanoparticles. Results are expressed as the mean ± SD (n=3).
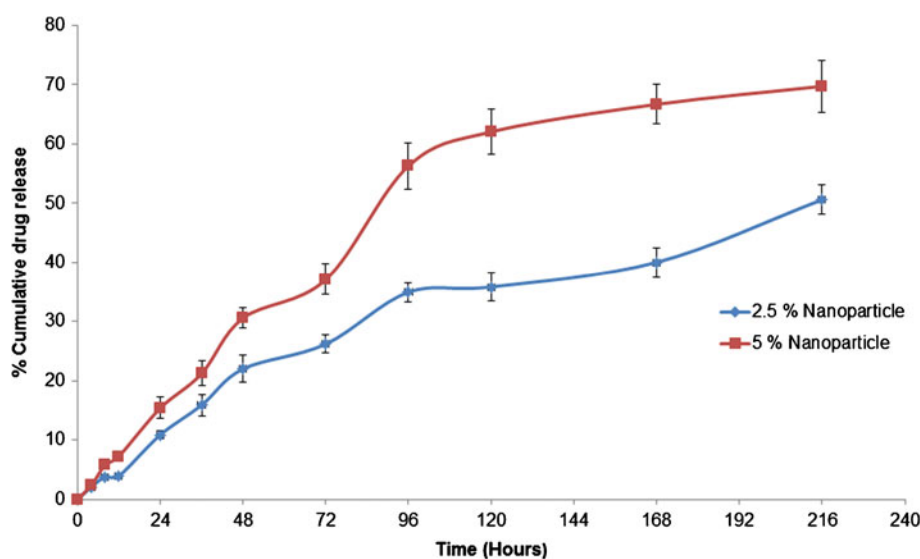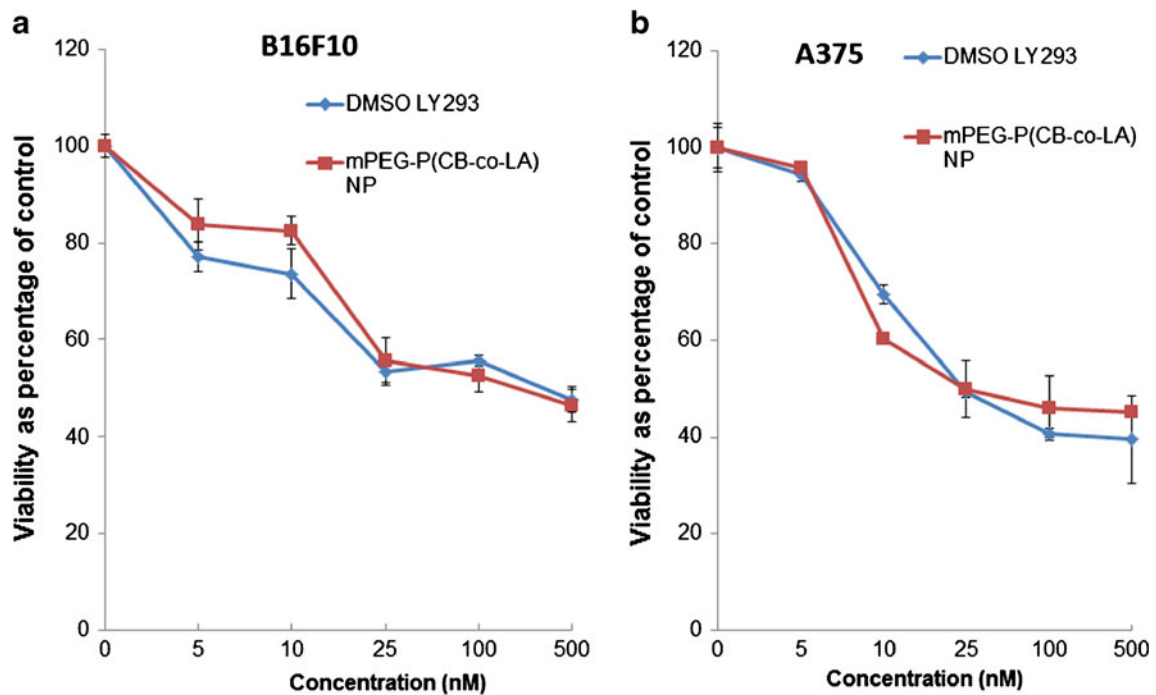
Fig. 5 Effect of DMSO solution of LY293 and drug loaded nanoparticles on (**a**) B16F10 and (**b**) A375 cell viability after 48 h of treatment. Cell viability was determined by MTT Assay and expressed as the % of control. Results are expressed as the mean ± S.D (n=4).

control group to $40.03 \pm 1.91\%$ in DMSO solution of LY293 and $38.95 \pm 0.17\%$ in LY293 nanoparticles group. By observing sub G1 peak, we also determined the effect of 48 h LY293 treatment on apoptosis of A375 cells.

Treatment with DMSO solution of LY293 and LY293 nanoparticles resulted in significant apoptosis as evident by remarkable increase in the percentage of cells in sub G1 phase (Fig. 7b).
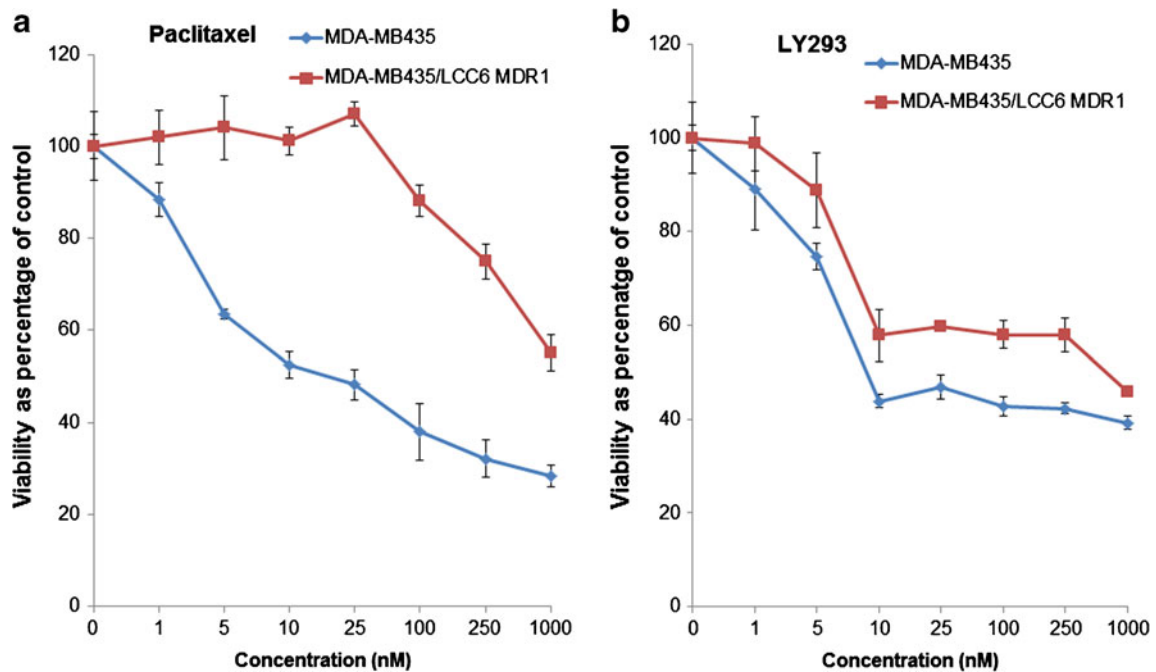

Fig. 6 Effect of paclitaxel and LY293 on cell viability of Pgp overexpressing melanoma cell. Cytotoxicity of paclitaxel (**a**) and LY293 (**b**) in MDA-MB435 and MDA-MB435/LCC6 MDR1 cells respectively after 48 h of treatment. Cell viability was determined by MTT Assay and expressed as % of control. Results are expressed as the mean ± SD (n=4).
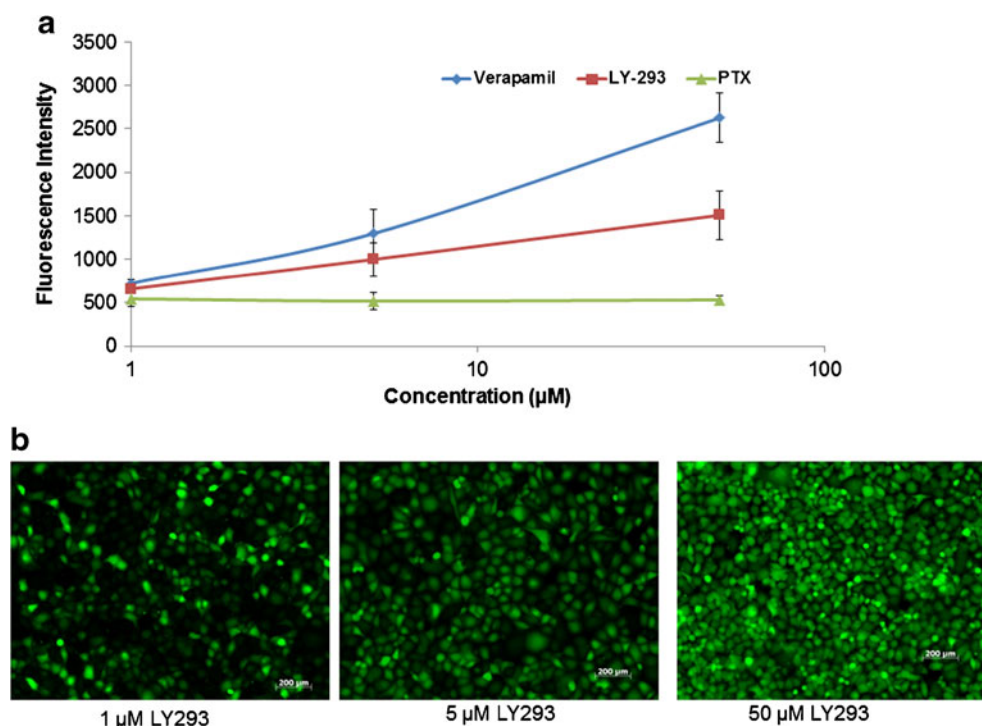
Fig. 7 Effect of LY293 on Pgp activity. (**a**) Intracellular calcein accumulation in MDA-MB435/LCC6MDR1 after 30 min treatment with Verapamil, LY293 and PTX. Results are expressed as the mean ± SE (n=3). (**b**) Fluorescent images depicting dose-dependent increase in intracellular calcein fluorescence in MDA-MB435/LCC6 MDR1 following 30 min treatment with LY293.

Effect of LY293 on Tubulin Polymerization

In our previous publication, we have shown that LY293 binds to tubulin and prevents polymerization (8). We confirmed the mechanism by performing immunofluorescence microscopy of β tubulin in drug treated A375 cells. Immunofluorescence images (Fig. 9d and e) clearly showed that treatment with LY293 dissolved in DMSO or encapsulated in nanoparticles inhibited β tubulin polymerization whereas treatment with paclitaxel as expected stabilized microtubules (Fig. 9).

DISCUSSION

Clinical use of paclitaxel, a microtubule stabilizer has shown significant improvement in treating various cancers including melanoma. However, prolonged treatment with paclitaxel is known to develop chemoresistance due to the overexpression of adenosine triphosphate–binding cassette (ABC) transporters (14,15). ABC transporters such as Pgp, multiple drug resistance protein (MRP) and breast cancer resistance protein (BCRP) lead to ATP dependent translocation of paclitaxel across biological membrane. To overcome the Pgp mediated multiple drug resistance (MDR), several strategies have been studied including co-administration of Pgp inhibitors, down-regulation of MDR genes, synthesis of novel compounds that

evade Pgp efflux and drug delivery approaches (16,17). Previously we have reported the use of Lapatinib to inhibit Pgp mediated efflux of paclitaxel (17). Drug delivery approaches including nanoparticles, liposomes, micelles and drug polymer conjugates have been used to overcome the Pgp resistance and this effect has been attributed to improved endocytic uptake of drug carriers (18–21). However, nanocarriers composed of surfactants like TPGS/Brij 78 effectively inhibited Pgp by depleting ATP and/or interacting with the Pgp binding sites (22). Formulation approaches resulted in only slight decrease in IC_{50} values in low/moderately expressing Pgp cell lines and therefore, it is critical to synthesize new compounds which can overcome MDR resistance. Herein, we report the formulation and characterization of potent (2-(1 H-Indol-5-yl) thiazol-4-yl) 3, 4, 5-trimethoxyphenyl methanone (LY293).

We have recently shown potent anticancer activity of LY293 in various cancer cells by inhibiting tubulin polymerization (8). To confirm the efficacy of this drug in MDR resistant cells, Pgp overexpressing MDA-MB435/LCC6 MDR1 melanoma cells were used in the present study. Resistance factor was calculated by dividing IC_{50} values of paclitaxel in MDR1 overexpressing MDA-MB435/LCC6MDR1 cell lines with IC50 in parental MDA-MB435 cell line. LY293 had similar potency in both resistant and nonresistant cells whereas paclitaxel had a resistance factor of 80 in MDA-MB435/LCC6 MDR1 (Fig. 6). To confirm the results of
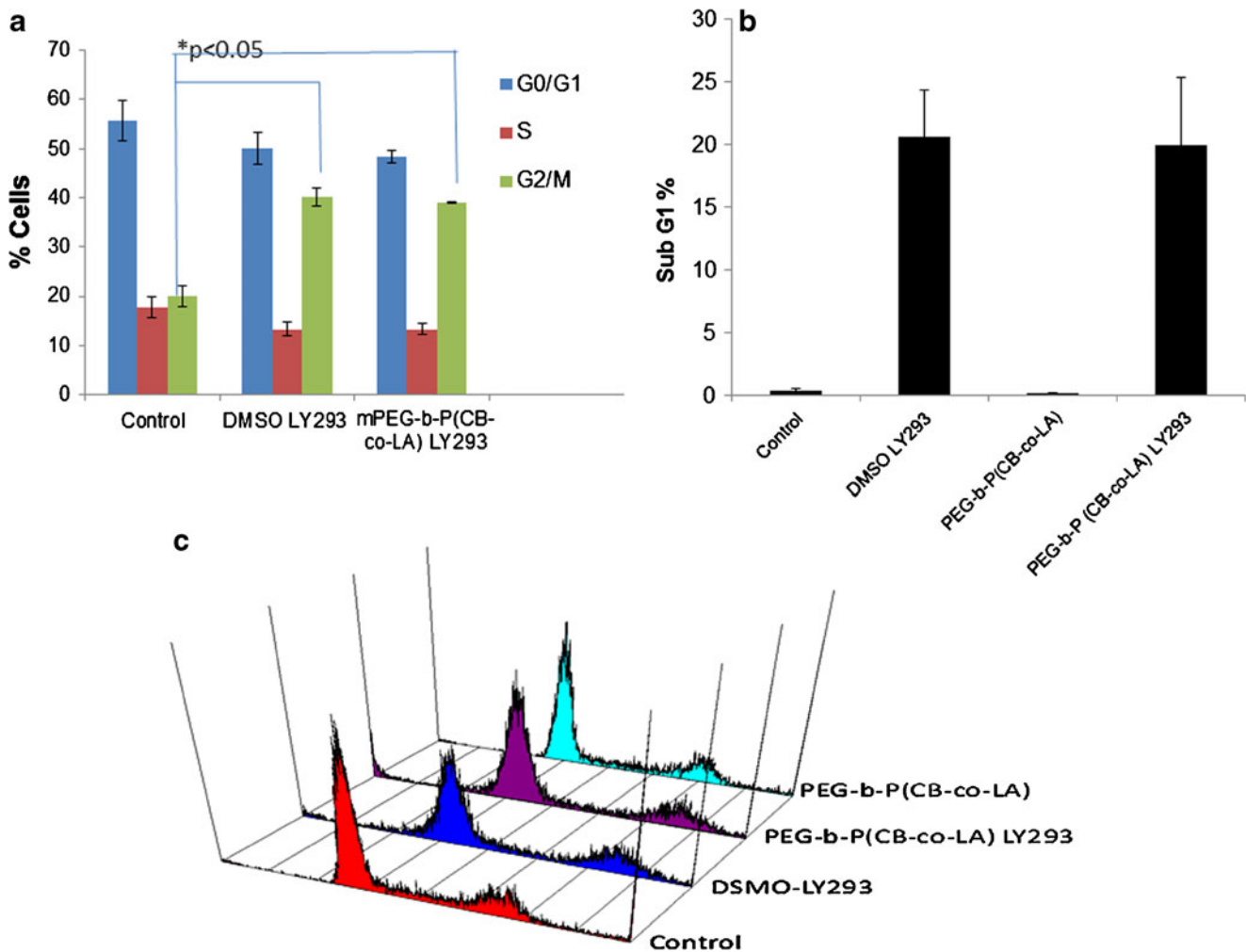
Fig. 8 Effect of DMSO solution of LY293 and nanoparticle formulation of LY293 on A375 cell cycle analysis and apoptosis. (**a**) Cell cycle distribution after 24 h of treatment with DMSO, LY 293 dissolved in DMSO, blank nanoparticle and drug loaded nanoparticle. *p < 0.05 using Student's unpaired *t* test. (**b**) Apoptosis of A375 cells after 48 h of treatment expressed as percent sub G1 cells. Results are expressed as the mean ± SD (n=3). (**c**) Histogram showing cell cycle distribution.

cytotoxicity in Pgp overexpressing cell line, we determined whether LY293 is a Pgp substrate. However, with our previous characterization of SMART 100 (which has similar structural scaffold) for Pgp inhibition, we presumed that LY293 would have Pgp inhibitory activity. To confirm our presumption, Calcein AM efflux assay was performed. Treatment with LY293 (Fig. 7) led to concentration dependent increase in intracellular fluorescence indicating the inhibition of Pgp by
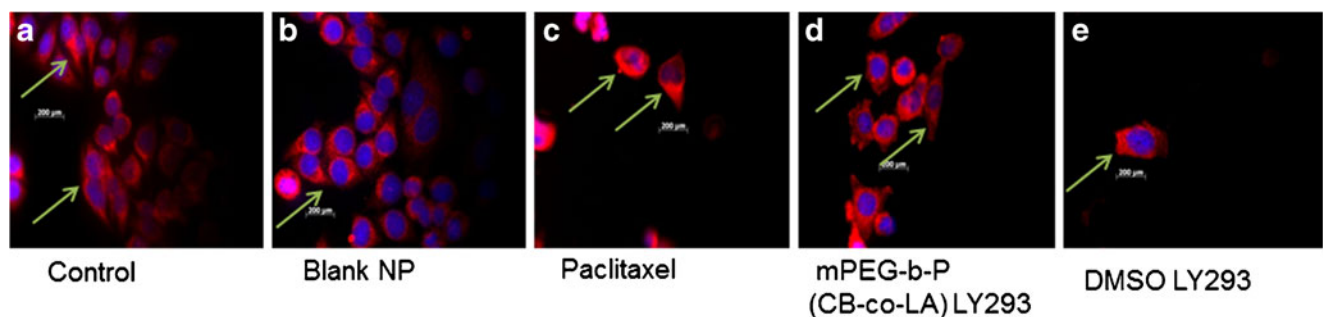

Fig. 9 Effect of LY293 treatment on tubulin polymerization. Immunofluorescence images showing tubulin immunostained with rabbit monoclonal anti-tubulin antibodies, followed by Dylight 594 secondary antibody (*red color*) and nucleus stained with DAPI (*blue color*). Arrows highlight the difference in cytoskeleton arrangement of cells upon treatment with (**a**) control, (**b**) blank NP (**c**) paclitaxel, (**d**) mPEG-b-P(CB-co-LA) LY293, and (**e**) DMSO LY293.

LY293. However, our previous studies have shown that 2 - aryl-4 benzoyl imidazoles (ABI) compounds do not modulate Pgp ATPase enzyme and thereby suggesting that ABI series of compounds are not Pgp substrate (23). Findings from these two assays do not corroborate as Pgp substrates/inhibitors modulate activity of ATPase enzyme. However, it is critical to note that Pgp substrates like colchicine and methotrexate do not modulate ATPase activity (24). Interestingly TPGS, a nonionic surfactant has also been shown to inhibit the efflux of Calcein AM but does not modulate ATPase activity (22). To further characterize the effect of LY293 on Pgp activity, assays like monolayer efflux studies and Pgp glow assay will be carried out in our future studies.

Secondly, poor aqueous solubility of LY293 limited its systemic administration. Therefore, we have synthesized mPEG-b-P (CB-co-LA) copolymer to prepare nanoparticles for delivery of this drug. Cytotoxicity of LY293 in melanoma cells was comparable to DMSO solution of free drug (Fig. 5). This result suggests that encapsulation of LY293 into mPEG b- P (CB-co-LA) nanoparticles did not diminish the inhibitory effect of LY293 on cell proliferation.

LY293 like other tubulin binding agents exerts its antimitotic effect by interfering with the progression of cell cycle at the early mitotic (G2/M) phase. Treatment with LY293 in DSMO or formulated in nanoparticles lead to cell cycle arrest in G2/M phase (Fig. 8a). This finding suggests that the chromosomes failed to segregate after replication, stalling the cell cycle at the metaphase checkpoint and allowing mitotic arrest. Subsequent to cell cycle arrest in G2/M phase, cells undergo apoptosis. Sub G1 fraction of propidium iodide stained cells was calculated to determine the extent of apoptosis. A375 cells exhibited significant apoptosis upon treatment with the formulations of LY293 (Fig. 8).

Drug acting on tubulin polymerization affects the microtubule structure of the cells undergoing division. This disruption of the normal microtubule structure was examined using immunofluorescence microscopy and results are shown in Fig. 9. LY293 prevented the polymerization of tubulin and resulted in the rearrangement of cytoskeleton structure. Control or the cells treated with blank nanoparticles showed normal microtubules, whereas paclitaxel treatment resulted in the stabilization of microtubules around nuclei. These immunofluorescence images of β tubulin have confirmed the mode of action of LY293.

In summary, we have formulated and characterized a potent microtubule destabilizing agent. mPEG-b-P (CB-co-LA) nanoparticles have shown excellent efficacy and induced apoptosis in melanoma cells. Considering the results, we are strongly encouraged to take forward mPEG-b-P (CB-co-LA) nanoparticles formulation of LY293 for *in vivo* studies as a potential therapy for melanoma.

REFERENCES

1. Balch CM, Soong S-J, Gershenwald JE, Thompson JF, Reintgen DS, Cascinelli N, *et al.* Prognostic factors analysis of 17,600 Melanoma patients: Validation of the American Joint Committee on Cancer Melanoma Staging System. J Clin Oncol. 2001;19(16):3622–34.

2. Gray-Schopfer V, Wellbrock C, Marais R. Melanoma biology and new targeted therapy. Nature. 2007;445(7130):851–7.

3. Serrone L, Zeuli M, Sega FM, Cognetti F. Dacarbazine-based chemotherapy for metastatic melanoma: Thirty-year experience overview. J Exp Clin Cancer Res. 2000;19(1):21–34. Epub 2000/06/07.

4. Leonard GD, Fojo T, Bates SE. The role of ABC transporters in clinical practice. Oncologist. 2003;8(5):411–24.

5. Sève P, Dumontet C. Is class III β-tubulin a predictive factor in patients receiving tubulin-binding agents? The Lancet Oncology. 2008;9(2):168–75.

6. Chen Z-S, Hopper-Borge E, Belinsky MG, Shchaveleva I, Kotova E, Kruh GD. Characterization of the transport properties of human Multidrug Resistance Protein 7 (MRP7, ABCC10). Mol Pharmacol. 2003;63(2):351–8.

7. Lu Y, Li C-M, Wang Z, Ross CR, Chen J, Dalton JT, *et al.* Discovery of 4-substituted methoxybenzoyl-aryl-thiazole as Novel Anticancer Agents: Synthesis, biological evaluation, and structure −activity relationships. J Med Chem. 2009;52(6):1701–11.

8. Lu Y, Li C-M, Wang Z, Chen J, Mohler ML, Li W, *et al.* Design, synthesis, and SAR studies of 4-substituted methoxylbenzoyl-aryl-thiazoles analogues as potent and orally bioavailable anticancer agents. J Med Chem. 2011;54(13):4678–93.

9. Gelderblom H, Verweij J, Nooter K, Sparreboom A, Cremophor EL. The drawbacks and advantages of vehicle selection for drug formulation. Eur J Cancer. 2001;37(13):1590–8.

10. Li F, Lu Y, Li W, Miller DD, Mahato RI. Synthesis, formulation and *in vitro* evaluation of a novel microtubule destabilizer, SMART-100. Journal of Controlled Release. 2010;143(1):151–8.

11. Danquah M, Li F, Duke C, Miller D, Mahato R. Micellar delivery of bicalutamide and embelin for treating prostate cancer. Pharm Res. 2009;26(9):2081–92.

12. Danquah M, Fujiwara T, Mahato RI. Self-assembling methoxypoly(ethylene glycol)-b-poly(carbonate-co-l-lactide) block copolymers for drug delivery. Biomaterials. 2010;31 (8):2358–70.

13. Panyam J, Williams D, Dash A, Leslie-Pelecky D, Labhasetwar V. Solid-state solubility influences encapsulation and release of hydrophobic drugs from PLGA/PLA nanoparticles. J Pharm Sci. 2004;93(7):1804–14.

14. Hodi FS, Soiffer RJ, Clark J, Finkelstein DM, Haluska FG. Phase II study of paclitaxel and carboplatin for malignant melanoma. Am J Clin Oncol. 2002;25(3):283–6.

15. Bedikian AY, Plager C, Papadopoulos N, Eton O, Ellerhorst J, Smith T. Phase II evaluation of paclitaxel by short intravenous infusion in metastatic melanoma. Melanoma Research. 2004;14(1):63–6.

16. Szakacs G, Paterson JK, Ludwig JA, Booth-Genthe C, Gottesman MM. Targeting multidrug resistance in cancer. Nat Rev Drug Discov. 2006;5(3):219–34.

17. Li F, Danquah M, Singh S, Wu H, Mahato R. Paclitaxel- and lapatinib-loaded lipopolymer micelles overcome multidrug resistance in prostate cancer. Drug Delivery and Translational Research. 2011;1(6):420–8.

18. Rahman A, Husain SR, Siddiqui J, Verma M, Agresti M, Center M, *et al*. Liposome-mediated modulation of multidrug resistance in human HL-60 leukemia cells. Journal of the National Cancer Institute. 1992;84(24):1909–15.

19. Minko T, Kopečková P, Pozharov V, Kopeček J. HPMA copolymer bound adriamycin overcomes MDR1 gene encoded resistance in a human ovarian carcinoma cell line. Journal of Controlled Release. 1998;54(2):223–33.

20. Han M, Diao Y-Y, Jiang H-L, Ying X-Y, Chen D-W, Liang W-Q, *et al*. Molecular mechanism study of chemosensitization of doxorubicin-resistant human myelogenous leukemia cells induced by a composite polymer micelle. Int J Pharm. 2011;420(2):404–11.

21. Ma P, Dong X, Swadley CL, Gupte A, Leggas M, Ledebur HC, *et al*. Development of idarubicin and doxorubicin solid lipid nanoparticles to overcome Pgp-mediated multiple drug resistance in leukemia. J Biomed Nanotechnol. 2009;5(2):151–61.

22. Dong X, Mattingly CA, Tseng MT, Cho MJ, Liu Y, Adams VR, *et al*. Doxorubicin and paclitaxel-loaded lipid-based nanoparticles overcome multidrug resistance by inhibiting P-glycoprotein and depleting ATP. Cancer Res. 2009;69(9):3918–26.

23. Wang Z, Chen J, Wang J, Ahn S, Li C-M, Lu Y, *et al*. Novel tubulin polymerization inhibitors overcome multidrug resistance and reduce melanoma lung metastasis. Pharm Res. 2012 Mar 13. doi:10.1007/s11095-012-0726-4.

24. Litman T, Zeuthen T, Skovsgaard T, Stein WD. Structure-activity relationships of P-glycoprotein interacting drugs: Kinetic characterization of their effects on ATPase activity. Biochim Biophys Acta (BBA) - Mol Basis Dis. 1997;1361(2):159–68.